

FAST SODIUM IMAGING AT 9.4 TESLA

Christian Mirkes^{1,2}, G. Shajan¹, and Klaus Scheffler^{1,2}

¹High-Field MR Center, Max Planck Institute for Biological Cybernetics, Tuebingen, BW, Germany, ²Department for Biomedical Magnetic Resonance, University of Tuebingen, Tuebingen, BW, Germany

PURPOSE

Sodium magnetic resonance imaging (sMRI) suffers from an inherently low signal-to-noise ratio (SNR) due to the physical properties of the sodium nucleus and the low concentrations found in the human body. In this study, several fast imaging techniques commonly used for proton imaging were adapted for sMRI and used at 9.4 T.

METHODS

All measurements were performed on a Siemens (Erlangen, Germany) 9.4 T human whole-body MR scanner. The sodium nuclei (105.7 MHz) were excited with a 4-channel transceiver array and the retransmitted NMR signal was acquired with a state-of-the-art 27-channel receive coil. Proton imaging (399.7 MHz) was performed with an integrated 4-channel proton dipole array¹.

An SNR comparison based on the pseudo replica approach² was performed for three spiral imaging sequences which used either RF spoiling, gradient spoiling (FISP—fast imaging with steady-state precession³) or balanced gradients (bSSFP—Steady-state free precession⁴). A total of 100 pseudo replica were generated for each measurement and used to create SNR maps. The sequence parameters of the used stack of spirals were chosen as follows: nominal resolution 1.5x1.5x4.0 mm³, partitions 52, spiral interleaves per partition 130, TR 10 ms, readout time 3 ms (RF spoiled acquisition and FISP) and 5 ms (bSSFP), acquisition time (TA) 10 min. The duration of the hard excitation pulse was set to 2 ms in order to achieve sufficient flip angle while adhering to the prescribed SAR limits. Owing to the spiral readout, an echo time of TE 1.6 ms could still be achieved.

The B_0 field distribution was mapped with a standard proton double-echo sequence: TE₁ 3.5 ms, TE₂ 4.3 ms, TR 300 ms, Slices 30, Res 2x2x2.5, TA 74 s. A phase-sensitive method⁵ was used to map the B_1 field generated by the sodium coil. It consisted of two acquisitions for which a hard 180° pulse rotating the magnetization either clock- or anticlockwise around the x-axis was followed by a 90° pulse around the y-axis. The used sampling scheme was a stack of spiral having the following imaging parameters: resolution 3x3x5 mm³, FoV 240 mm, 40 partitions, TE 3 ms, TR 200 ms, TA 6 min. An intensity correction⁶ was performed for the sodium images acquired with the 27-channel receive coil based on a homogeneous reference image acquired with the 4-channel transceiver array.

RESULTS

The B_0 and B_1 maps for several transversal slices are shown in Figures 1&2. A flip angle of roughly 40° was achieved for the central slices. The images produced by the three fast imaging sequences are displayed in Figures 3a-c. The intensity correction and the reduced sensitivity of the 27-channel array in the center of the brain led to a slight but still acceptable noise enhancement in that area. The bSSFP images exhibit excellent image quality and only a few banding artefacts can be seen in the vitreous humor of the eye (indicated by a red arrow in Figure 3c). The corresponding SNR maps are shown in Figures 3d-f. The relative SNR measured in a large region of interest (ROI) in a central slice was: 42 (spoiled acquisition), 44 (FISP), and 56 (bSSFP), respectively.

DISCUSSION & CONCLUSION

Even though the sodium nucleus possesses very short transverse and longitudinal relaxation times, bSSFP imaging still allows to increase SNR and hence image quality. Considering the high spatial resolution that can be achieved with steady state imaging sequences at ultra-high field compared to sodium density imaging, it may be worthwhile investigating the usefulness of these imaging techniques in case of brain tumors and other pathologies.

REFERENCES

1. Shajan et al. Proceedings ISMRM-ESMRMB 2014;22:620
2. Robson et al. Magn. Reson. Med. 2008;60:895–907.
3. Hawkes and Patz. Magn. Reson. Med. 1987;4:9–23.
4. Scheffler et al. Eur Radiol 2003;13:2409–2418.
5. Allen et al. Magn. Reson. Med. 2011;65:1125–30.
6. Pruessmann et al. Magn. Reson. Med. 1999;42:952–62.

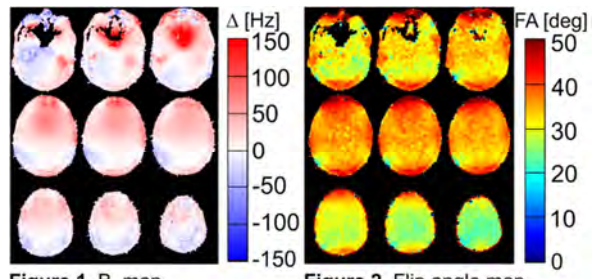


Figure 1. B_0 map.

Figure 2. Flip angle map.

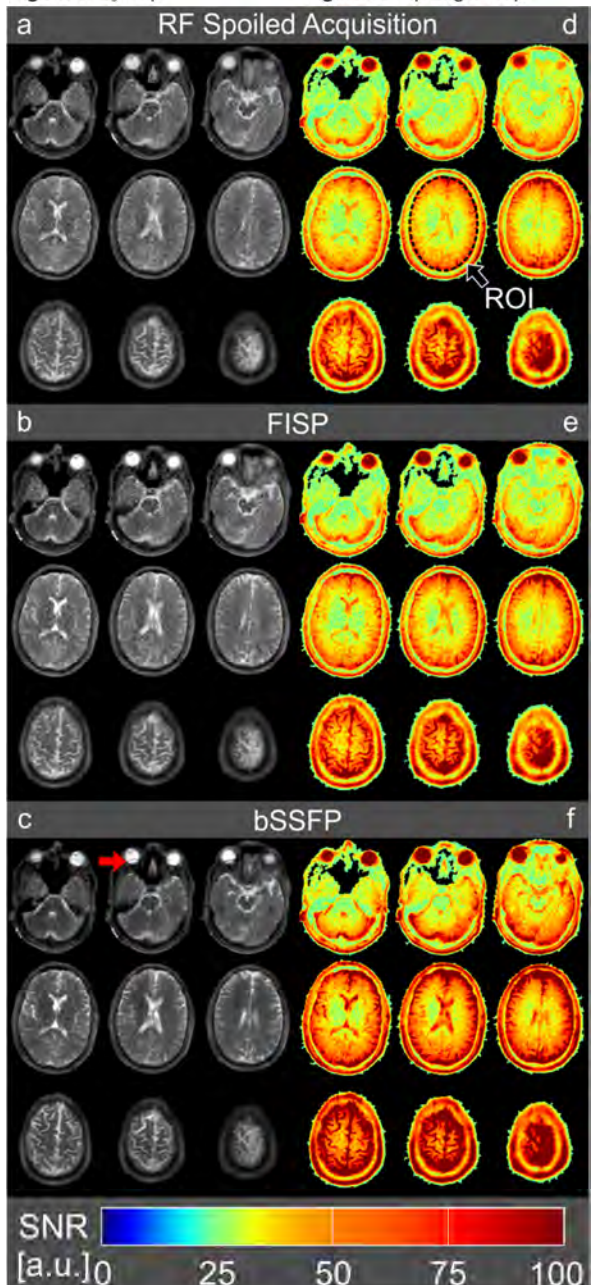


Figure 3. In vivo images (a-c) and corresponding relative SNR maps (d-f) acquired with different spoiling schemes.